Progress In Electromagnetics Research M, Vol. 39, 1–9, 2014

An Analysis of Near-field Scattering Characteristics of Rough Target: From the Perspective of Bidirectional Reflectance Distribution Function Based on LS-SVM

Ning Li, Min Zhang*, Ding Nie, and Wangqiang Jiang

Abstract—The near-field scattering characteristics of rough target are analyzed by using a revised bidirectional reflectance distribution function (BRDF) of a rough surface based on least squares support vector machine (LS-SVM). The revised BRDF is more reliable in a larger range of incident angles and scattering angles that beyond the scope of experimental measurements. The basic principle of LS-SVM and the modeling process are firstly introduced in detail. Then the comparison among LS-SVM, the back propagation neural network (BPNN) and the measured data is carried out. The results show that the LS-SVM model has better integrative performance, stronger generalization ability and higher precision. On this basis, the calculation of the near-field radar cross section (RCS) of a complex target is safely performed and analyzed. The method proposed is helpful to better investigate the near-field scattering characteristics of rough target.

1. INTRODUCTION

Generally speaking, it is difficult to calculate the near-field scattering characteristics of rough surfaces. But the bidirectional reflectance distribution function (BRDF) can reflect the optical scattering properties of rough surfaces. It is a critical means to studying the complex laser and infrared light scattering properties. Based on the direct functional relationship between BRDF and the laser radar cross section (LRCS) per unit area, BRDF has been receiving great attention for its myriad applications in research areas such as target detection and recognition, stealth technology and so on [1, 2]. If the reliable BRDF can be obtained in various angle configurations, it will be applied to analyzing the near-field scattering characteristics. Thus, how to get the reliable BRDF will be the primary issue that should be solved.

There are two primary approaches to studying the BRDF, namely, theoretical calculation [3] and experimental measurement [4, 5]. The former needs to obtain the roughness statistical parameters of rough surfaces, and then carry out calculations based on light scattering theory of rough surfaces. Due to the complexity of theoretical calculations and the difficulty to directly obtain the roughness parameters of various materials, experimental measurement is more frequently used in engineering applications. In the laboratory bright sources of light are used to measure the BRDF of sample surfaces, and laser beams are used as sources because of their high brightness, convenience, and availability. But an experiment can be carried out only in a limited range of incident angles and scattering angles, thus, the BRDF model is developed by using the experimental data of different materials to acquire the corresponding BRDF values of the incident angles and scattering angles that can not be easily measured in actual experiment.

There are various ways to establish a BRDF calculation model, such as the geometrical optics theory-based Cook-Torrance model [6], the modified Phong model [7], the Ward model [8] and the Oren-Nayar model [9]. However, most of them are for irregular surfaces which are difficult to be simulated.

Received 8 May 2014, Accepted 14 September 2014, Scheduled 23 September 2014
* Corresponding author: Min Zhang (mzhang@mail.xidian.edu.cn).
The authors are with the School of Physics and Optoelectronic Engineering, Xidian University, Xi'an 710071, China.

Recently, in view of the automation of the fitting function's selection, two methods have been proposed: artificial neural network (ANN) [10] and support vector machine (SVM) [11]. ANN is for large-sampled data and SVM for small-sampled data. They use kernel function to solve various problems, avoiding selecting the fitting function, which enables the method to be more versatile. However, as a new machine learning approach for small-sampled data developed based on statistics theory, SVM has many unique advantages over ANN in some engineering fields [12].

Using the structural risk minimization principle instead of the empirical risk minimization principle, SVM has the advantages of simple structure, global optimization and strong generalization ability, which makes it a hot spot of the machine learning research. However, the major drawback of SVM is its high computational burden and low training efficiency because of the required constrained optimization programming. With regard to this problem, a new method to establish the BRDF model by Least Squares Support Vector Machine (LS-SVM) is proposed in this paper. While keeping the main merits of standard SVM, LS-SVM has the advantages of simple calculation, high calculation speed and little memory requirement [13], which has a great potential for future application in the calculation of target scattering properties.

The paper is organized as follows. The principle of LS-SVM is mainly introduced in Section 2. On this basis, Section 3 presents the establishment of BRDF model for arbitrary incident angles and scattering angles by appropriately choosing the kernel function and model parameters. The simulated results are shown and analyzed successively in Section 4. Then, the near-field scattering properties of complex target are calculated based on BRDF, and the results are provided in Section 5. Section 6 concludes this paper.

2. THE PRINCIPLE OF LS-SVM

The LS-SVM [14, 15] is a new type of SVM proposed by J. A. K. Suykens in 1999, which can be seen as a development and improvement of standard SVM. The LS-SVM converts the inequality constraints of standard SVM into equality ones, which leads to solving a linear system instead of a quadratic programming problem. Moreover, the number of the unknown parameters of the LS-SVM model built with Radical Basis Function (RBF) is only two, less than those of standard SVM, which greatly simplifies the problem. As a result, the convergence performance is obviously enhanced and the solving process is greatly accelerated. Thus the algorithm is described in detail as follows [16].

Considering a scattered dataset of N points $\{x_k, y_k\}_{k=1}^N$, with n-dimensional input data $x_k \in R^n$ and output data $y_k \in R$, we can define linear equation of higher dimensional feature space:

$$y = \varphi(x)\omega^T + b \tag{1}$$

where the nonlinear mapping $\varphi(\cdot)$: $R^n \to R^{n_k}$ maps the input data into a so-called high-dimensional feature space (which can be infinite-dimensional), $\omega \in R^{n_k}$ is weighed value vector and $b \in R$ is threshold value. Consequently, the problem of fitting pluralistic nonlinear model can be transformed into linear regressive problem. The optimization problem is replaced by the following equations [17]:

$$\begin{cases} \min\limits_{\omega,b,e} J(\omega, e) = \dfrac{1}{2}\omega^T\omega + \dfrac{1}{2}\gamma\sum\limits_{k=1}^{N} e_k^2 \\ s.t.\ y_k = \omega^T\varphi(x_k) + b + e_k, \quad k = 1, 2, \ldots, N \end{cases} \tag{2}$$

where the first term stands for the minimization of the Vapnik Chervonenkis (VC) dimension, while the second one minimizes the training errors (e_k). The regularization constant $\gamma > 0$ is included to control the bias-variance trade-off.

Note that in some cases, ω becomes infinite dimension, and the above formulation cannot be used to solve the problem. Therefore, we need to perform the computations in another space, called the dual space of Lagrangian multipliers after applying Mercer's theorem [18]. Consider the Lagrangian of Eq. (2) given by:

$$L = J(\omega, e) - \sum_{k=1}^{N} \alpha_k \left(\omega^T\varphi(x_k) + b + e_k - y_k\right) \tag{3}$$

Here $\alpha = (\alpha_1, \alpha_2, \ldots, \alpha_l), \alpha_i \in R$ are Lagrangian multipliers. By Karush-Kuhn-Tucker (KKT) optimal conditions [19], the first order conditions for optimality are given by:

$$\begin{cases} \dfrac{\partial L}{\partial \omega} = 0 \rightarrow \omega = \displaystyle\sum_{k=1}^{N} \alpha_k \varphi(x_k) \\ \dfrac{\partial L}{\partial b} = 0 \rightarrow \displaystyle\sum_{k=1}^{N} \alpha_k = 0 \\ \dfrac{\partial L}{\partial e_k} = 0 \rightarrow \alpha_k = \gamma e_k \\ \dfrac{\partial L}{\partial \alpha_k} = 0 \rightarrow \omega^T \varphi(x_k) + b + e_k - y_k = 0 \end{cases} \qquad k = 1, 2, \ldots, N \tag{4}$$

Eq. (4) can be written successively as the solution to the following set of linear equations

$$\begin{bmatrix} I & 0 & 0 & -\varphi(x_n) \\ 0 & 0 & 0 & -1_n \\ 0 & 0 & \gamma I & -I \\ \varphi(x_n)^T & 1_n & I & 0 \end{bmatrix} \begin{bmatrix} \omega \\ b \\ e \\ \alpha \end{bmatrix} = \begin{bmatrix} 0 \\ 0 \\ 0 \\ y \end{bmatrix} \tag{5}$$

After eliminating ω, e from the equations, combining with Mercer conditions $K(x_k, x_l) = \varphi(x_k)^T \varphi(x_l)$, we obtain:

$$\begin{bmatrix} 0 & 1_n^T \\ 1_n & \Omega + \gamma^{-1} I \end{bmatrix} \begin{bmatrix} b \\ \alpha \end{bmatrix} = \begin{bmatrix} 0 \\ y \end{bmatrix} \tag{6}$$

where $y = [y_1, \ldots, y_N]^T$, $1_n = [1, \ldots, 1]^T$, $\alpha = [\alpha_1, \ldots, \alpha_N]^T$, $\Omega = K(x_k, x_l)$, $k, l = 1, 2, \ldots, N$, I is an identity matrix. From Eq. (6), the regression parameters b and α can be solved as

$$b = \frac{1_n^T (\Omega + \gamma^{-1} I_n)^{-1} y}{1_n^T (\Omega + \gamma^{-1} I_n)^{-1} 1_n} \tag{7}$$

$$\alpha = \left(\Omega + \gamma^{-1} I_n\right)^{-1} (y - 1_n b) \tag{8}$$

Thus, the regression function is expressed in dual form as

$$y(x) = \sum_{k=1}^{N} \alpha_k K(x_k, x) + b \tag{9}$$

3. THE ESTABLISHMENT OF BRDF MODEL

Given a training data set $\{x_k, y_k\}_{k=1}^N$, here $x_k \in R^n$ are n influencing factors of the BRDF values and $y_k \in R$ are measured values of BRDF, the modeling procedure is expressed as follows.

(a) Divide the samples into two parts: the training data that is used to build up the model and the test data that is used to test the model generalization capability.

(b) Select appropriate kernel function and parameters and train the samples with the LS-SVM regression algorithm. Calculate the support vector α and the corresponding threshold b using Eq. (7) and Eq. (8), then establish the LS-SVM data processing model.

(c) Obtain the fitting and forecasting results by substituting the input data into the LS-SVM model. If the results meet the actual needs, the process stops. Otherwise, go to step (b) to adjust the corresponding parameters of the regression model and recalculate the results, until they could meet the requirement.

3.1. The Choice of Kernel Function

Kernel function is the core of SVM. The choice of kernel function will greatly influence the learning ability and generalization ability of machine learning. Different kernels determine different nonlinear transformations and characteristics spaces, thus selecting different kernels to train SVM will lead to different results. Any function $K(x_i, x_j)$ satisfying Mercer's condition can be used as the kernel function. Thus different kernel functions possess their respective traits, and exert varying degrees of influences on recurrent LS-SVM performance. Among these functions, the RBF function can map the sample set from the input space into a high-dimensional feature space effectively, which is helpful for representing the complex nonlinear relationship between the output and input samples. Based on this, the RBF function is used widely. In this paper, RBF function is also selected as the kernel function, which is expressed as follows:

$$K\left(x_i, x_j\right) = e^{-||x_i - x_j||^2/\sigma^2} \tag{10}$$

3.2. The Choice of the Model Parameters

As a very important part in LS-SVM modeling, the choice of parameters directly affects the accuracy of data fitting, generalization ability as well as the training speed. For a specific problem, inappropriate parameters may lead to unexpected results of data fitting and forecasting.

Due to the selection of RBF as the kernel function, it can be seen that there are two free parameters, regularization parameter γ and kernel width parameter σ, that have to be properly optimized. The first parameter γ determines the trade-offs between the minimization of the fitting error and the minimization of the model complexity. For the definite dataset, a small value of γ denotes a slight penalty on the experience error, a low complexity of the learning machine and a high experience risk, which is called "under-fitting". The bigger of the γ value, the longer the training time will be. But too big a value of γ will cause over-fitting and decline of the generalization ability. The second parameter σ mainly affects the complexity of the distribution of samples in high-dimensional feature space. The fitting error will decrease as the value of σ gets small, but too small a value of σ could also cause over-fitting. In order to obtain a pair of superior parameters, we have to change the parameters and carry on the training for many times. Finally the parameters of the learning machine are acquired according to all the previous test results. There could be several parameter selection methods such as cross-validation type method [20], leave-one-out method, grid-search method and three-step-search method [21]. In this paper we use the three-step-search method.

4. MODELING RESULTS AND ANALYSIS

The material used for modeling and testing in this paper is a kind of paint and the wavelength of the incident light is 0.905 μm. Here, the measured data of BRDF has four influencing factors $(\theta_i, \varphi_i, \theta_s, \varphi_s)$, these four angles are respectively denoted as incident angle, incident azimuth, scattering angle and scattering azimuth. The sample data are obtained within the following angle range: $\theta_i \in [30°, 90°]$ with a sampling interval of 5°, φ_i is fixed to 20°, $\theta_s \in [5°, 175°]$ with a sampling interval of 1° and $\varphi_s \in [10°, 90°]$ with a sampling interval of 10°. The above data are divided into two categories: test sample data and training sample data, and the test sample data are chosen in the angle range of $\theta_i = 45°$ and 75°, $\varphi_i = 20°$, $\theta_s \in [5°, 90°]$ and $\varphi_s \in [10°, 90°]$.

After several adjustments, the optimal values of γ and σ^2 are 1513.0 and 48.0 respectively for the LS-SVM model and the following calculation results shown in Fig. 1 and Fig. 2. Moreover, the back propagation neural network (BPNN) [22] fitting data are also provided to be compared with those obtained by LS-SVM in Fig. 1 and Fig. 2. BPNN is a popular neural network algorithm with wide applications, which has the main advantage that it can minimize the error sum of square between the actual data and the desired data. The root mean square error (RMSE) is used to evaluate the effect.

$$E_{RMSE} = \sqrt{\frac{\sum_{i=1}^{N} \left|y_i - y_i'\right|^2}{N}} \tag{11}$$

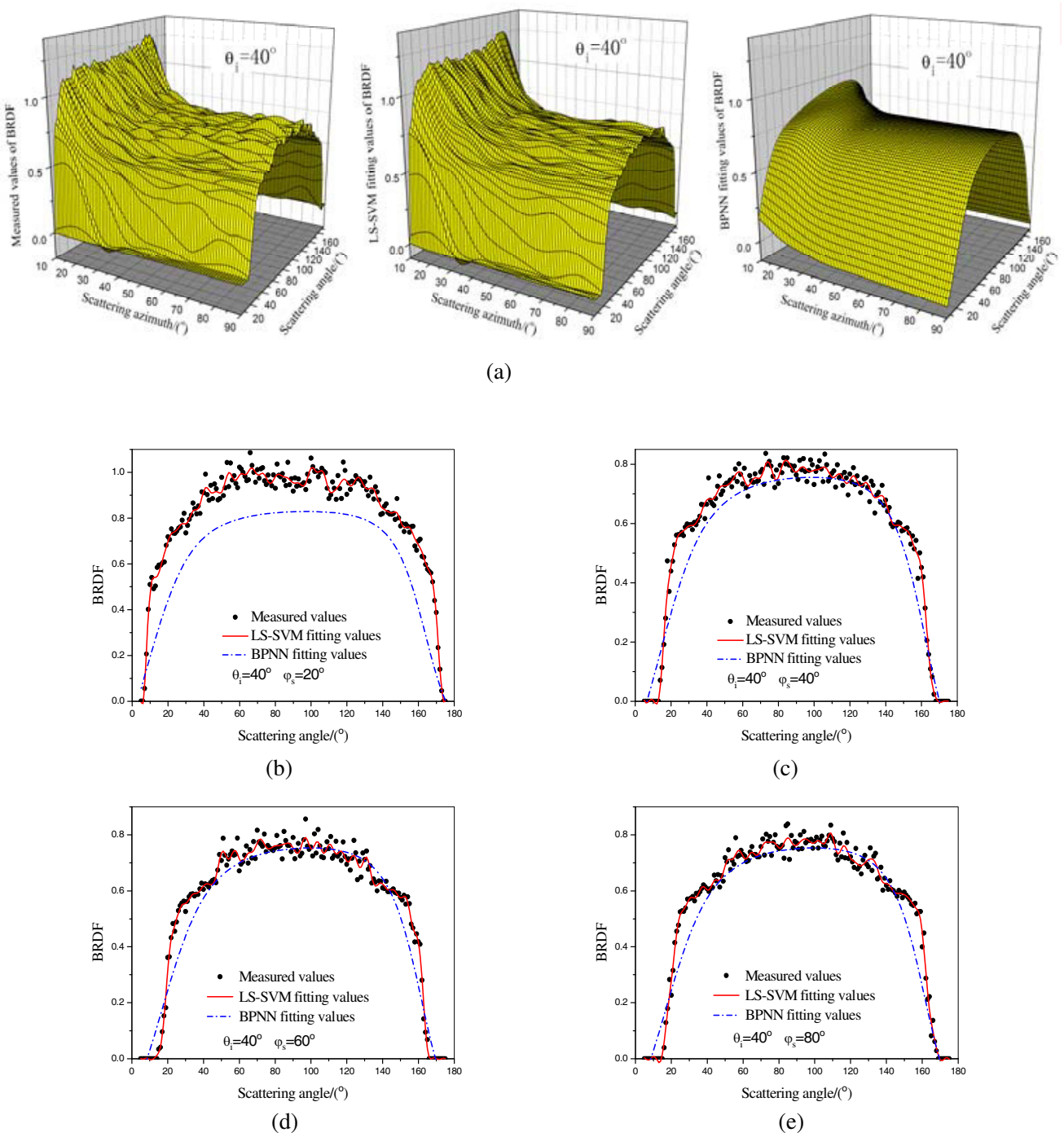

Figure 1. Comparison between measured values and fitting values with $\theta_i = 40°$ (The values of θ_i participate in the training). (a) 3D distribution of the measured BRDF data, LS-SVM fitting BRDF data and BPNN fitting BRDF data (from left to right). (b) $\varphi_s = 20°$. (c) $\varphi_s = 40°$. (d) $\varphi_s = 60°$. (e) $\varphi_s = 80°$.

N is the number of the sample, y_i the forecasting data of each sample, and y_i' the measured value.

From the comparisons shown in Fig. 1 and Fig. 2, we can see that both the LS-SVM model's fitting data and forecasting data agree with the measured data with smaller errors and higher precision. Moreover, with regard to E_{RMSE}, the LS-SVM forecasting sample has a value of 0.0578 and the BPNN

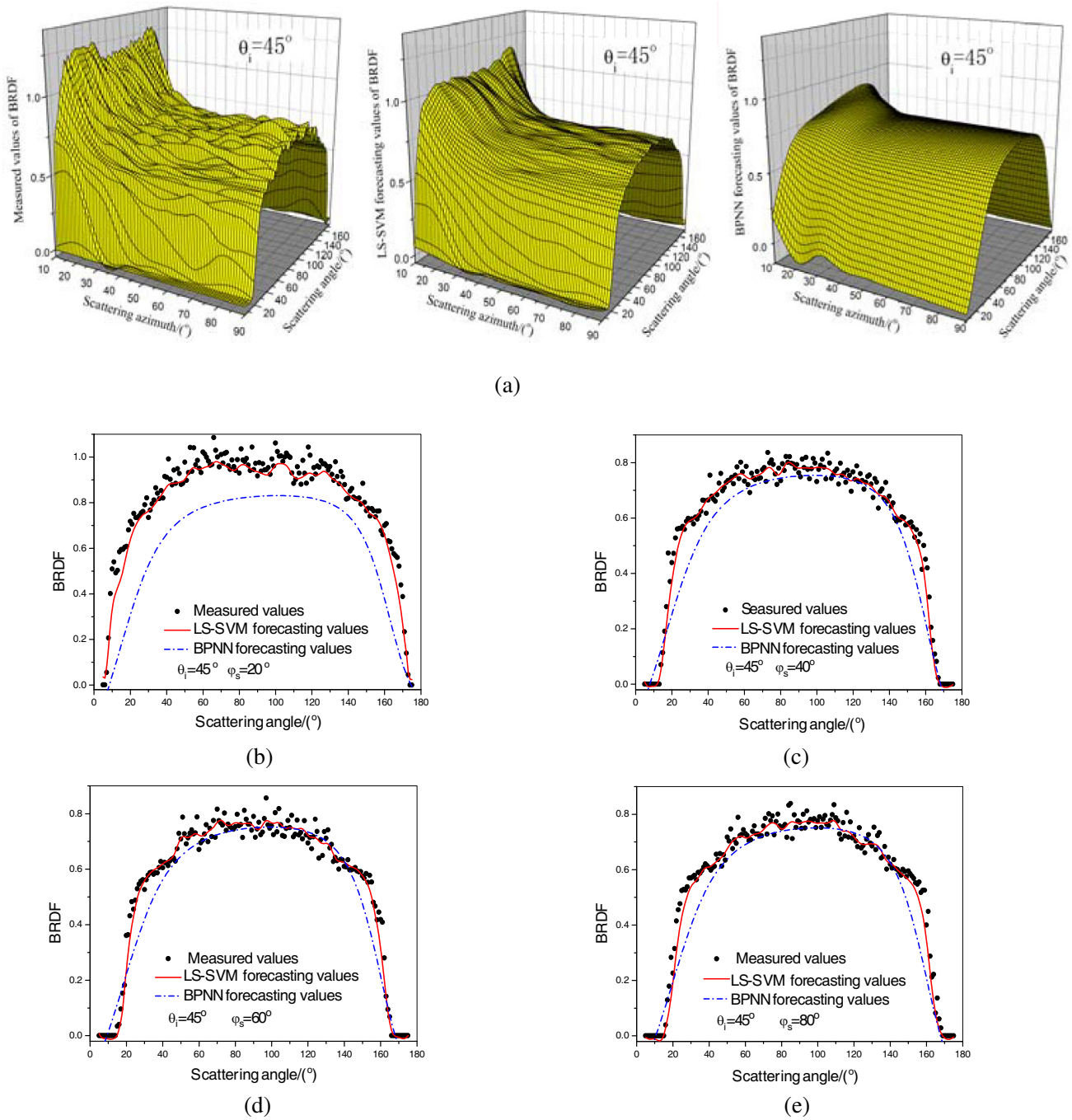

Figure 2. Comparison between measured values and forecasting values with $\theta_i = 45°$. (The values of θ_i don't participate in the training). (a) 3D distribution of the measured BRDF data, LS-SVM forecasting BRDF data and BPNN forecasting BRDF data (from left to right). (b) $\varphi_s = 20°$. (c) $\varphi_s = 40°$. (d) $\varphi_s = 60°$. (e) $\varphi_s = 80°$.

forecasting sample has a value of 0.1704. Therefore LS-SVM has obvious improvement compared with BPNN. This indicates that LS-SVM is more accurate and has higher generalization ability. Based on the analysis above, the data obtained by LS-SVM method can be safely applied to the calculation of near-field scattering properties of target.

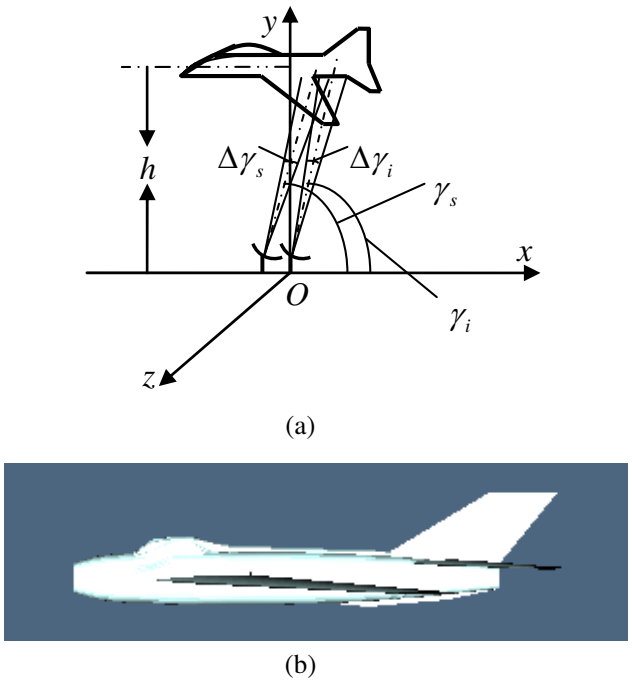

Figure 3. The schematic diagram of calculating scattering characteristics of the target.

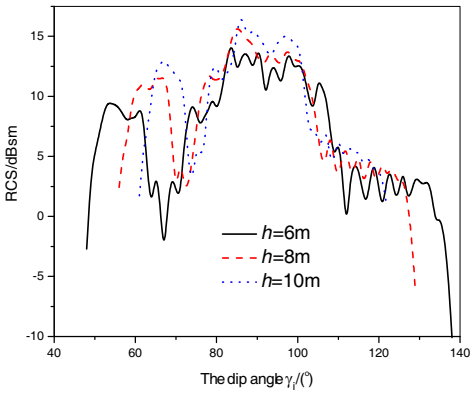

Figure 4. RCS of the target changes with the dip angle γ_i.

5. THE APPLICATION OF LS-SVM IN CALCULATING NEAR-FIELD SCATTERING CHARACTERISTICS OF COMPLEX TARGET

Figure 3(a) shows the schematic diagram of calculating the near-field scattering characteristics of the target. The whole target relative to the emitter is in the near-field region. The laser only illuminates a small portion of the target at a time, and the surface of effective irradiated area can be dissected into small triangle facets. These facets can be characterized by their node coordinates, area sizes and normal vectors. Each surface facet relative to the emitter is in the far-field region and can be studied by using far-field method [23]. The echo power of each facet can be expressed as

$$\Delta P_s = \frac{P_i \Delta s \sigma^0}{4\pi \cos\theta_i} \lim_{R_l \to \infty} \frac{A_r}{R_l^2} \tag{12}$$

where P_i is the power of each facet intercepted, Δs the area of each facet, σ^0 the average value of the RCS per unit area, θ_i the incident angle, R_l the range between the detector and the facet, and A_r the aperture area of the detector.

In the other formulation entailing the BRDF, the echo power is

$$\Delta P_s = f_r P_i \Delta s \cos\theta_s \lim_{R_l \to \infty} \frac{A_r}{R_l^2} \tag{13}$$

f_r is the BRDF at incident angle θ_i and scattering angle θ_s. By comparing Eq. (12) and Eq. (13), we get

$$\sigma^0 = 4\pi f_r \cos\theta_i \cos\theta_s \tag{14}$$

Combining Eq. (14) and the effective irradiation area, the RCS of the whole target can be obtained.

In this paper, we use the Gaussian-beam wave model [24] for calculation. h denotes the distance from the detector to the target, the width of the transmitting beam (denoted by $\Delta\gamma_i$) is 3° and the angle between the beam and x-axis is denoted by γ_i. The distance that from the detector to the emitter is 0.03 m. The width of the receiving beam (denoted by $\Delta\gamma_s$) is also 3°, and the angle between it and x-axis is γ_s. The target to be analyzed here is a simulated geometrical model of a plane with a length

of about 12.5 m, a height of about 3 m and a width of about 9 m, as is illustrated in Fig. 3(b), assuming the surface of the plane is coated with the paint that used in the experiment in Section 4.

Here, the site of the target is fixed. The angle of γ_i changes gradually from 0° to 180°, and the angle of γ_s is always two degrees larger than γ_i. The variation of RCSs with the dip angle γ_i is simulated and shown in Fig. 4, in which the emitter is supposed to be 10 m, 8 m and 6 m below the target respectively. The results show that the RCS peaks appear on the wings and the empennages. This may be due to the fact that the irradiation area is larger in these two parts. Moreover, the value of the peaks rises with the increase of height h.

6. CONCLUSIONS

This paper presents a new attempt to evaluate the laser scattering properties of complex targets in the near-field region based on the revised BRDF model of rough surface materials. It is worth noting that the revised BRDF model is reliable in a relatively larger range of incident angles and scattering angles by using the LS-SVM. The comparison of the measured data and the forecasting values just verifies the LS-SVM model. On this basis, the calculation of the near-field RCS of a complex target is safely performed and analyzed. Although the calculation of RCS presented in this work is only limited to a plane-like target, the outline and corresponding conclusions will help to better investigate the near-field scattering characteristics of rough targets from the perspective of BRDF. Future work will be carried out to study the near-field scattering characteristics of much more complex targets by using the revised BRDF based on LS-SVM.

ACKNOWLEDGMENT

The authors would like to thank the Fundamental Research Funds for the Central Universities and the National Natural Science Foundation of China under Grant Nos. 41306188 and 61372004 to support this kind of research.

REFERENCES

1. Gibbs, D. P., C. L. Betty, A. K. Fung, and A. J. Blanchard, "Automated measurement of polarized bidirectional reflectance," *Remote Sensing of Environment*, Vol. 43, 97–114, 1993.
2. Li, H. K., N. Pinel, and C. Bourlier, "A monostatic illumination function with surface reflections from one-dimensional rough surfaces," *Waves in Random and Complex Media*, Vol. 21, 105–134, 2011.
3. Ulaby, F. T., R. K. Moore, and A. K. Fung, *Microwave Remote Sensing*, Addison-Wesley, New York, 1982.
4. Arai, K., "Method for estimation of grow index of tealeaves based on Bi-directional reflectance distribution function: BRDF measurements with ground based network cameras," *International Journal of Applied Sciences*, Vol. 2, 52–62, 2011.
5. Jordan, D. L., "Experimental measurements of optical backscattering from surfaces of roughness comparable to the wavelength and their application to radar sea scattering," *Waves in Random and Complex Media*, Vol. 5, 41–54, 1995.
6. Cook, R. L. and K. E. Torrance, "A reflectance model for computer graphics," *Computer Graphics*, Vol. 15, 307–316, 1981.
7. Phong, B. T., "Illumination for computer generated pictures," *Communications of the ACM*, Vol. 18, 311–317, 1975.
8. Ward, G. J., "Measuring and modeling anisotropic reflection," *Computer Graphics*, Vol. 26, 265–272, 1992.
9. Oren, M. and S. K. Nayar, "Generalization of the Lambertian model and implications for machine vision," *International Journal Computer Vision*, Vol. 14, 227–251, 1995.

10. Li, W., J. F. Chen, and T. Wang, "Prediction of the plasma distribution using an artificial neural network," *Chinese Physics B*, Vol. 18, 2441–2444, 2009.
11. Vapnik, V., E. Levin, and Y. Le Cun, "Meaning the VC-dimension of a learning machine," *Neural Computation*, Vol. 6, 851–876, 1994.
12. Balabin, R. M. and E. I. Lomakina, "Support vector machine regression (SVR/LS-SVM)-an alternative to neural networks (ANN) for analytical chemistry? Comparison of nonlinear methods on near infrared," *Analyst*, Vol. 136, 1703–1712, 2011.
13. Wang, H. F. and D. J. Hu, "Comparison of SVM and LS-SVM for regression," *International Conference on Neural Networks and Brain*, Vol. 1, 279–283, 2005.
14. Suykens, J. A. K. and J. Vandewaiie, "Least squares support vector machine classifiers," *Neural Processing Letter*, Vol. 9, 293–300, 1999.
15. Suykens, J. A. K., T. V. Gestel, J. D. Brabanter, B. D. Moor, and J. Vandewalle, *Least Squares Support Vector Machines*, World Scientific Publishers, Singapore, 2002.
16. Adankon, M. M., M. Cheriet, and A. Biem, "Semisupervised learning using Bayesian interpretation: Application to LS-SVM," *IEEE Transactions on Neural Networks*, Vol. 22, 513–524, 2011.
17. Gestel, V., et al., "Financial time series prediction using least squares support vector machines within the evidence framework," *IEEE Transactions on Neural Networks*, Vol. 12, 809–821, 2001.
18. Scholkopf, B. and S. Mika, "Input space vs. feature space in Kernel based methods," *IEEE Trans. on Neural Networks*, Vol. 10, 1000–1017, 1999.
19. Fletcher, R., *Practical Methods of Optimization,* John Wiley and Sons, Chichester and New York, 1987.
20. Browne, M. W., "Cross-validation methods," *Journal of Mathematical Psychology*, Vol. 44, 108–132, 2000.
21. Guo, H., H. P. Liu, and L. Wang, "Method for selecting parameters of least squares support vector machines and application," *Journal of System Simulation*, Vol. 18, 2033–2036, 2006.
22. Hecht-Nielsen, R., "Theory of the backpropagation neural network," *International Joint Conference on IEEE*, 93–605, 1989.
23. Tomiyasu, K., "Relationship between and measurement of differential scattering coefficient and bidirectional reflectance distribution function (BRDF)," *IEEE Transactions on Geoscience and Remote Sensing*, Vol. 26, 660–665, 1988.
24. Andrews, L. C., M. A. Al-Habash, C. Y. Hopen, and R. L. Phillips, "Theory of optical scintillation: Gaussian-beam wave model," *Waves in Random and Complex Media*, Vol. 11, 271–291, 2001.